Core Characterization of Patterson #5-25 Well for Carbon Capture and Storage in Western Kansas

Thomas Paronish[1,2*], *Rhiannon* Schmitt[1,3], *Dustin* Crandall[2], *Franek* Hasiuk[4], *Eugene* Holubnyak[4], *Jingyao (Jenny)* Meng[5]

[1] National Energy Technology Laboratory
[2] NETL Support Contractor
[3] Oak Ridge Institute for Science and Education
[4] Kansas Geological Survey
[5] Virginia Division of Geology and Mineral Resources

Abstract. The computed tomography facilities and the Geotek Multi-Sensor Core Logger at the National Energy Technology Laboratory were used to collect data and characterize core from the Patterson #5-25 well. The Patterson #5-25 well was drilled as part of the Kansas Geological Survey led Carbon Storage Assurance Facility Enterprise (CarbonSAFE) Phase 2 project, the Integrated Midcontinent Stacked Carbon Storage Hub. As part of the CarbonSAFE project, permeability measurements of selected core were measured in zones of interest. Beyond the initial project work, we characterized the lithology utilizing non-destructive qualitative (multiscale CT images) and quantitative (X-ray fluorescence, P-wave velocity, gamma density, magnetic susceptibility) techniques to better characterize the reservoir quality and seal potential within the cored intervals. The core from the Patterson #5-25 well includes nearly 625 feet of core intermittently between the Pennsylvanian Atoka Shale and into Precambrian Basement. Core logger data and coarse resolution CT images were taken from 2/3 slab core along the entire length of the core. In addition to this macroscopic characterization of the core, potential reservoir facies along the length were examined at ten locations with high resolution CT images to examine reservoir pore systems and structural properties such as fractures. The Pennsylvanian Morrow Sandstone and Cambrian Reagan Sandstone had the best reservoir quality with high porosity and permeability. The Pennsylvanian Atoka Shale had the best seal potential with low permeability and few fractures. Throughout the Cambro-Ordovician Arbuckle Group zones of good reservoir conditions via secondary porosity were observed, with intervals of sub-mm to cm-scale vuggy porosity separated by relatively tight dolomitic zones. The Meramecian, Osage, and Viola carbonate units were observed to have generally thinner zones of good reservoir quality with some small baffles.

1 Introduction

The increase of CO_2 in the atmosphere has caused the climate to change and it has been essential to understand and develop ways to reduce atmospheric CO_2 [1]. The Integrated Midcontinent Stacked Carbon Storage Hub (IMSCS-HUB) was designed to develop a commercial-scale carbon capture, utilization, and storage project as part of a Phase II Carbon Storage Assurance Facility Enterprise (CarbonSAFE) project. The IMSCS-HUB is made up of ethanol, power plants, and other sources in Iowa, Kansas, and Nebraska and three stacked storage corridors: Sleepy Hollow Field (southwest-central Nebraska), Madrid (southwest Nebraska), and Patterson Site (Patterson, Heinitz, Hartland, and Oslo fields) (western Kansas) (Fig. 1) [2,3]. The Patterson site's Patterson #5-25 well is the focus of this study.

Understanding of the lithology, storage properties, and seal potential of the formations involved in this project is essential for optimized and environmentally safe long-term storage. By utilizing petrophysical logs, multi-scale CT imaging, and core characterization a multi-pronged understanding of these rocks has been developed.

1.1 Site Background

The Patterson #5-25 well was drilled in the spring of 2020 in the Patterson Field and with 625 feet of core recovered from target intervals between the Atoka to Precambrian Basement. A detailed breakdown of the cored intervals is available in Table 1[2]. The Patterson Field, which was discovered in 1941 and still active has produced 3.14 Mbbls of oil from the Morrow Sand [4].

The Patterson Field sits atop a structural high within the Hugoton Embayment, that allows for four-way closure of the reservoir strata [2,3]. Initial estimates of storage potential following phase I showed the Patterson Field site could store up to 50Mt of CO_2 over 25 to 30 years based on simulations for storage in the Osage, Viola, and Arbuckle, and 200 Mt over the same period with the investigation of cored wells and seismic data in Phase II [2-4].

Table 1. Patterson #5-25 cored intervals and primary lithologies

Group/Formation	Cored depth (ft)	Primary lithology
Atoka Stage	4,615 to 4,751	Shale
Morrowan Stage (Morrow Sand)	4,751 to 4,880	Mixed (sand, shale, limestone)
Meramecian Stage	4,880 to 4,957	Limestone
Osage Stage	5.380 to 5, 439	Limestone
Viola Formation	5,640 to 5,719	Limestone
Upper Arbuckle (Jefferson City-Cotter Fm.)	5,780 to 5,826	Dolomite
Lower Arbuckle (Roubidoux Fm and Bonneterre Fm.)	5,959 to 6,200	Dolomite

* Corresponding author: thomas.paronish@netl.doe.gov

Reagan Sandstone and Granite wash	6,214 to 6,273	Sandstone
Precambrian Basement	6,278 to 6,300	Granite

The primary objective of this study is to build on the classification of the Patterson #5-25 well core utilizing non-destructive methods at NETL to understand the stratigraphy and sedimentology of reservoir units.

2 Methods

2.1 Core Characterization

The 625 feet of Patterson #5-25 Well core was examined and characterized to understand the lithologies present in the well and their storage potential. This was done by utilizing non-destructive experimental techniques at the NETL, which included core petrophysical measurements using a Geotek Multi-Sensor Corelogger and medical computed tomography (Medical CT) of the entire core length as well as micro-computed tomography (Micro-CT) image at selected reservoir zones. This data was compared to core data from the Kansas Geologic Survey (KGS) that includes porosity and permeability data and petrophysical logs (triple combo and NMR from Xaminer® Magnetic Resonance derived porosity and permeability). Halliburton estimated permeability at 6-inch intervals by utilizing the Coates Method with T2 peaks obtained from NMR. While details of this methodology are not provided, these permeability estimates are utilized for comparative analysis in the current work. Core-derived measurements were also provided by Premier Oilfield Group. Permeability and porosity were calculated from both full diameter core and core-plugs throughout the cored intervals and average permeability is displayed in log-plots [2]. The results show a discrepancy between the Coates modelled and core-measured permeability, in these cases the authors have more confidence in the core-measured result being it is a direct measure.

2.1.1 Multi-Sensor Core Logger (MSCL)

The MSCL provides core petrophysical measurements at high spatial resolution. The measurement suite includes gamma density, p-wave velocity, magnetic susceptibility, and X-Ray Fluorescence (XRF). This paper focuses on selected elements for the XRF and gamma density, and the data is available through the Energy Data eXchange portal [5].

The Patterson 5-25 Well was sampled using the MSCL at 6 cm resolution for the entire 625 feet of core. XRF data was collected using a portable handheld Olympus Delta Innov-X with a two-beam acquisition method at 60s exposure per beam. The two-beam mode provides a broad suit of elements including majors (Al, Si, P, S, Cl, Mg, K, and Ca), transition metals (Ti, Cr, Mn, Fe, Co), and trace metals (V, Ni, Cu, Zn, As, Mo, Ag, Cd, Sn, Sb, Hf, W, Pb, and Bi). We focus on major elements related to the dominant mineralogy which are shown on log plots as a percent of the total weight.

Gamma density was acquired by exposing the sample to gamma radiation and measuring the radiation attenuation. The attenuation is directly proportional to the density of the sample and is acquired by measuring the difference between radiation energy at the emission source and after it passes through the sample [6].

2.1.2 Medical CT images

Core scale CT scanning was done with a Toshiba® Aquilion TSX-101A/R medical scanner. The Medical CT generates images with a resolution in the mm-range, with a voxel resolution of 0.43 x 0.43 mm in the XY plane and 0.5 mm along the Z-axis. Scans were captured at energies of 135 KeV and 80 KeV. Radiographs are processed into a 3-D volumes and 2-D slices in ImageJ. For this study, the 2-D images were cropped to highlight the variation in the grayscale throughout the well.

Two CT scanning energies were used to enable determination of density using methods established in Siddiqui and Khamees, 2004; further details of the methodology used here can be found in Moore et al. (2018) [6,7]. Three homogenous standards with known bulk densities, similar to the core being interrogated, were used for calibration. Bulk density, or dual energy density was calculated using,

$$\rho_B = mCTN_{low} + pCTN_{high} + q \quad (1)$$

where [m, p, and q] are unknown coefficients that can be solved by setting up a system of equations with four 3x3 determinants and CTN are the CT numbers obtained at the low and high energies from the Medical CT [8].

In this study, the high and low energy images were processed by a Python script with a three dimensional 2-sigma gaussian blur to reduce noise. The scipy library in Python was used to solve for the m, p and q unknowns based on the calibration CTN values, which are then used to determine the ρ_B of each pixel in the 3-D volume. Any material with a density <1.5 g/cm^3 was removed from determination of average density along the core length, which was calculated using the image processing program ImageJ [9].

2.1.3 Micro CT images

Micro-CT scans were acquired using a ZEISS Xardia MicroXCT-400 CT scanner. Micro-CT images are higher resolution scans that allow for more detailed investigation of mineralogy and porosity. Five micro-CT scans were acquired at a 2.36 μm^3 voxel resolution. A small selection of samples were acquired in representative zones due to prolonged scanning times. Samples are listed in Table 2 and were 1-2 mm in diameter.

Table 2. Micro-CT images

Depth (ft)	Formation

4,771.30	Morrow Sand
5,812.40	Upper Arbuckle/ Jefferson City-Cotter Fm
5,972.12	Lower Arbuckle/Roubidouix Fm.
6,213.50	Bonneterre-Reagan Sand Boundary
6,222.60	Reagan Sand

2.1.4 Ilastik thresholding

The five micro-CT images in Table 2 where segmented into relevant components using Ilastik, which is a supervised machine learning software that utilizes user training to determine feature classes based on a feature vector: color/intensity, edge type, and texture [10]. Training images is a time-intensive process where the user determines classes and identifies representative features in these, until uncertainty is adequately minimized between classes. For this study, feature classes were chosen to represent pore space (air) and mineralogical features (including quartz, dolomite, feldspar, and high attenuating minerals). Not all classes were used for every image and each image was trained on the feature classes separately due to different mineralogical compositions. Additionally, pre-processing of the Micro-CT images occurred in ImageJ prior to training to optimize the threshold results, which included a three-dimensional 2-sigma gaussian blur and adjustment of gray-scale levels.

Post-threshold images were brought back into ImageJ where a Look Up Table was applied to highlight the feature classes, and a histogram was calculated to show the distribution of feature classes within a Region of Interest (ROI) and subsequently give the porosity for the sample based on the percent of air within the sample.

3 Results and Discussion

Core characterization of the Patterson #5-25 well is separated into 3 zones designated spatially based on the continuously cored intervals, these include zone 1, the Atoka Stage, Morrowan Stage, and Meramecian Stage; zone 2, the Osage Stage, Viola Limestone, and Upper Arbuckle; and zone 3, the Lower Arbuckle, Reagan Sandstone, and Granite wash. These zones are classified based on petrophysical and geochemical characteristics with a focus on high quality reservoir features shown via the 5 micro-CT images and segmentations.

3.1 Core Characterization Zone 1: Atoka, Morrow, and Meramecian

Zone 1 represents the Pennsylvanian Atoka, Pennsylvanian Morrow, and Mississippian Meramecian stratigraphy (Fig. 1). The Atoka Stage is made up of interbedded black shale and mudstone to wackestone (sometimes dolomitic). The Atoka has generally low permeability with some silty intervals exceeding 0.1 mD with similarly high porosity (10 to 20%). Although the Atoka Stage has 2-to-10-foot zones with increased porosity/permeability, the more dominant low permeability zones are comprised of approximately 30-foot intervals of black shale and tight limestones which act as low permeability seals.

The Morrowan Stage (4,751 to 4,880 ft) is comprised of a quartz-dominated medium- to coarse-grained sandstone and was oil-stained. Some pyrite can be seen throughout with some small interbedded mudstone and shale intervals. The base of the cored interval shows signs of increased amounts of shale, and logs show that this gradational effect continues to the top of the Meramacian Stage strata.

The Meramecian Stage strata (4,880 to 4,957 ft) is made up of primarily limestone with a small brecciation mudrock section. The limestone interval of the Meramecian stage was tight with little to no porosity or permeability but those vuggy sections did have significant porosity and permeability. The Meramecian is an ideal seal as it is comprised of massive tight carbonates with no local signs of vertical fractures.

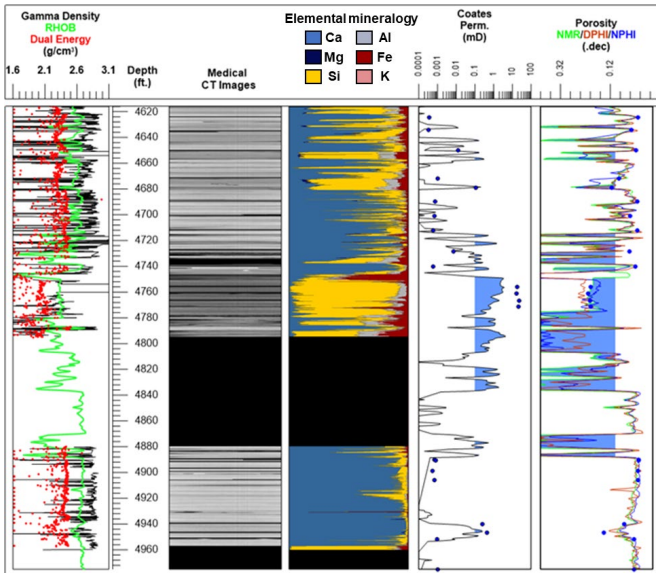

Fig. 1. Zone 1 log plot. Column 1 density (gamma density (black), dual energy density(red) and bulk density (green)); column 2, medical CT images; column 3, elemental mineralogy; column 4, Coates Permeability (line, fill represents zones of permeability greater than 0.1 mD) and core-derived permeability from KGS (dots)[2]; and column 5, porosity log (neutron porosity (NPHI, blue), density porosity (DPHI, red), NMR porosity (green, fill represents zones of porosity greater than .1)) and core-derived porosity from KGS (dots)[2].

3.1.2 Micro CT images

The micro-CT image for zone 1 was taken from the Morrow Stage which showed the best reservoir conditions in zone 1. Fig. 2. shows the results of the Ilastik threshold; a sample composition with 71.4% quartz, 7.2 % feldspar, and 1.7% high density minerals (including dolomite/calcite), with a porosity of 19.6%. The Morrow consists of generally well-sorted quartz with sub-angular to angular grains. Some quartz grains show intragranular fracturing which likely adds to the

overall porosity. Porosity in this sample mirrors the logs and KGS laboratory measurements for the sampled section. The feldspar grains are sparse but well sorted and show some intragranular fracturing similar to the quartz. The high-density mineral fraction was the lowest fraction of the volume analyzed and was mostly made up of pyrite and carbonate minerals.

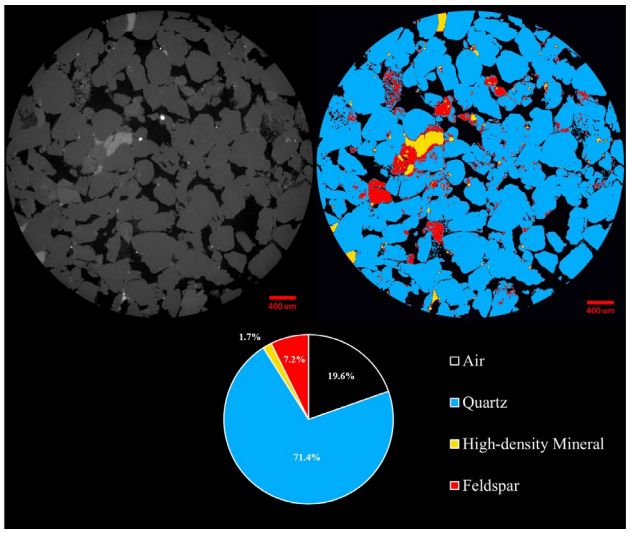

Fig. 2. Morrow sand micro-CT image with a slice of the volume showing the CT image unprocessed on left and threshold results on right (400 µm scale is shown on the bottom right of both images); below is the breakdown of feature classes from the volume.

3.2 Core Characterization Zone 2: Osage, Viola, and Upper Arbuckle

Zone 2 is represented by the Mississippian Osage Stage, Ordovician Viola Formation, and Upper Arbuckle (Jefferson City-Cotter Formations).

The Mississippian Osage Stage (5,380 to 5,439 ft) is made up of primarily limestone, with the upper 12 feet of core made up of a cherty limestone (seen in core and by the lack of clay elements (Al, Fe) and the enrichment of Si) (Fig. 3). This interval has excellent seal potential with porosities at about 5% or less and permeabilities less than 0.1 mD.

The Ordovician Viola Formation (5,640 to 5,720 ft) is the start of the Dolomitic dominated strata which continues to the base of the well (Fig. 4). The Viola Formation is made up primarily of dolopackstone in the upper portion of the formation with vugs and some mineralized fractures (5,640 to 5,654 ft) and brecciated intervals and chert-filled fractures and vugs at the bottom of the Viola Formation (5,658 to 5,720 ft). Vugs in the upper section of the Viola are open with some pin-point porosity becoming chert filled in the upper portion of the breccia. Porosity and permeability measurements from core and petrophysical logs show the Viola has between 5 to 10% porosity and 0.05 to 0.1 mD permeability (Fig.4), suggesting the Viola Formation would make a good reservoir unit.

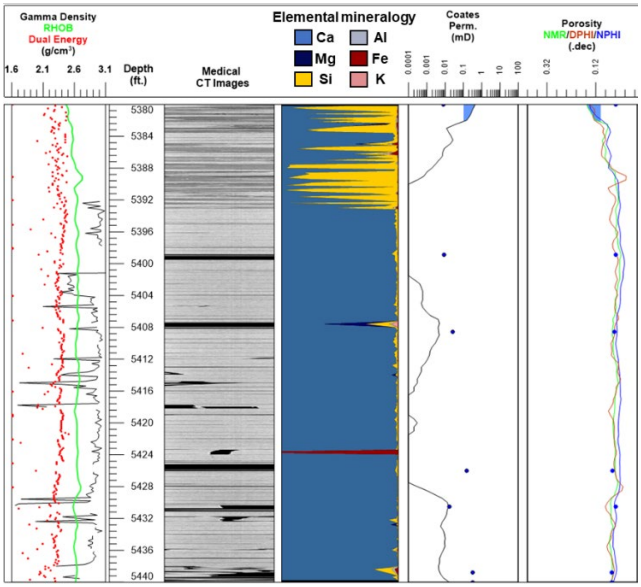

Fig. 3. Zone 2 Osage Stage log plot. See Fig. 1 for plot details

The Cambrian-Ordovician Upper Arbuckle (5,780 to 5,826 ft) is made up of the Jefferson City and Cotter Formations (Fig. 5). The Upper Arbuckle is primarily made up of Dolomite ranging between dolomudstone to dolograinstone. The dolomudstone intervals are generally tighter with some chert-filled vugs, and the dolograinstone have more porous features like vugs and pin-point porosity features. The Upper Arbuckle is also a good reservoir zone with an average porosity of about 9% and permeability between 0.01 and 0.1 mD.

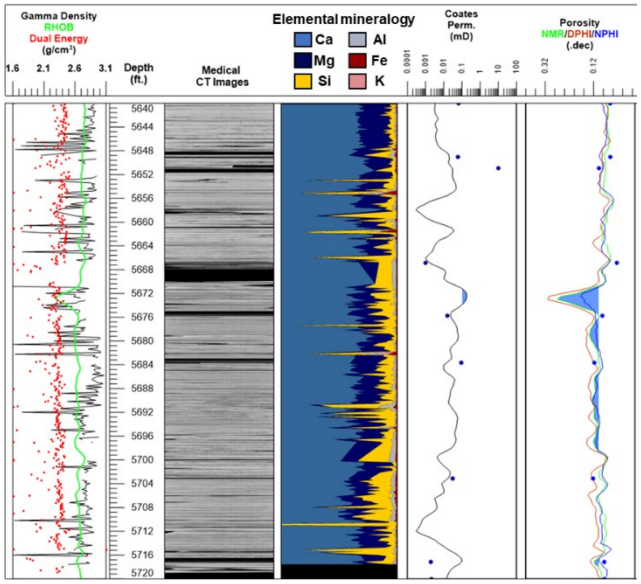

Fig. 4. Zone 2 Viola Stage log plot. See Fig. 1 for plot details

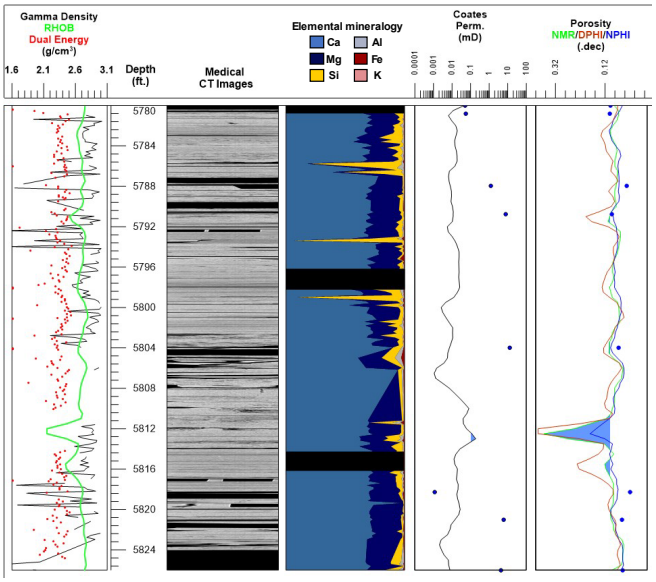

Fig. 5. Zone 2 Lower Arbuckle log plot. See Fig. 1 for plot details

3.2.1 Micro CT images

The sample examined with micro-CT in zone 2 was from the Upper Arbuckle (Jefferson City-Cotter Formation) at 5,812.4 ft (Fig. 6). This sample showed the best reservoir conditions in zone 2 and was taken from a section of dolograinstone with vuggy porosity surrounding the sample. The Ilastik segmentation shows the sample composition was dolomite and very minor amounts of high attenuating minerals (likely pyrite), with a porosity of 4.6%. The segmentation results miss some minor amounts of high-density minerals and quartz/feldspar grains; however, they are minor (<1%).

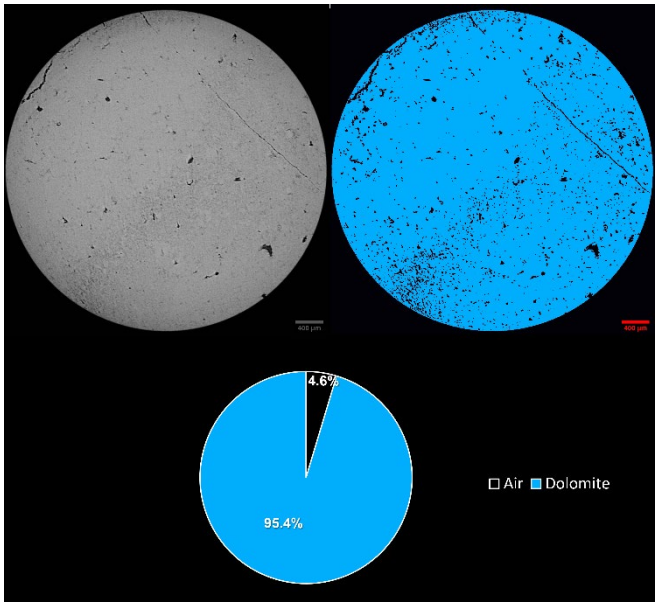

Fig. 6. Upper Arbuckle micro-CT image with a slice of the volume showing the CT image unprocessed on left and segmentation results on right (400 µm scale is shown on the bottom right of both images); below is a pie chart representing the portions of feature classes from the volume.

3.3 Zone 3: Lower Arbuckle, Reagan, and Granite wash

Zone 3 is made up of the Lower Arbuckle subgroup that includes the Roubidouix and Bonneterre formations, the Reagan Sandstone, and Granite wash (Fig. 7). The Lower Arbuckle subgroup is made of primarily of dolomitic facies. The Roubidoux Formation (5,959 to 6,042 ft) is made up of dolomudstone, dolograinstone, and doloboundstones. The dolomudstone intervals are generally tight with some vuggy porosity and open fractures, whereas the doloboundstone and dolograinstone facies contain more vuggy porosity and are highly fractured (mostly mineralized). At 6,016 to 6,025 ft, the Roubidoux becomes a sandy dolostone where the porosity increases to about 12% and permeability to about 10 mD.

The Bonneterre Formation (6,042 to 6,216 ft) is made up of dolomudstone and doloboundstone, both tighter than the Roubidoux Formation. Doloboundstone intervals are fractured with mineralized calcite. Doloboundstone in the lower portion of the formation were vuggier and more porous. The Bonneterre has more range in porosity (from 1 to 9%) and permeability (0.001 to 0.98 mD) but did show good reservoir characteristics.

The Reagan Sandstone and Granite wash (6,214 to 6,273 ft) consists of medium to fine-grained sandstones, siltstone, and conglomerates with mm- to cm-sized quartz clasts. The Reagan Sandstone portion (6,214 to 6,259 ft) is more dolomitic compared to the Granite wash interval (6,259 to 6,273 ft), which contains more feldspars and less dolomite. These intervals show good reservoir characteristics with porosity and permeability ranges between 9 to 15% and 0.01 and 2 mD.

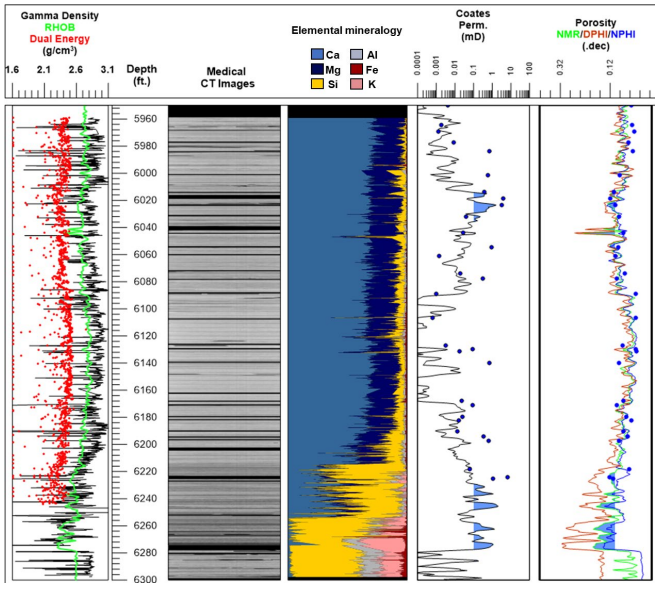

Fig 7. Zone 3 log plot. See Fig. 1 for plot details

3.3.1 Micro CT images

The micro-CT images examined in zone 3 were from the Lower Arbuckle (Roubidoux) at 5,972.12 ft (Fig. 8); Bonneterre-Reagan Sandstone boundary at 6,213.50 ft (Fig. 9); and from medium-grained sandstone from the Reagan

Sandstone at 6,222.60 ft (Fig. 10). All were chosen because they were representative sections of these zones in the core and log data.

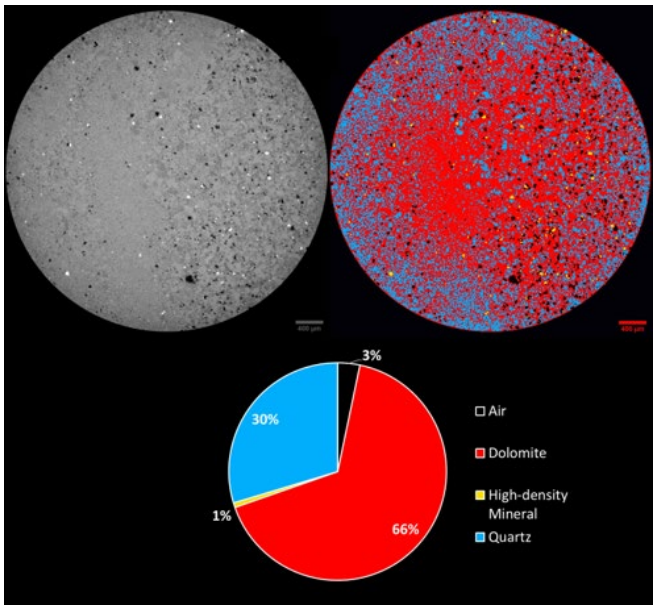

Fig. 8. Lower Arbuckle (Roubidoux) micro-CT image (5,972.12 ft) with a slice of the volume showing the CT image unprocessed on left and segmentation results on right (400 µm scale is shown on the bottom right of both images) and below a pie chart representing the portions of feature classes from the volume.

The Lower Arbuckle (Roubidoux) at 5,972.12 ft (Fig. 8) was sub sampled in a dolomudstone facies that was within some visible porosity zones. The Ilastik segmentation results, ignoring the outer 350 µm due to beam-hardening effects, show that the sample is primarily made up of dolomite (66%), lighter minerals (likely a combination of quartz, feldspar, and clay minerals) (30%), and high-density minerals (1%) with a porosity of 3%, slightly lower than the log derived porosity. Both the CT image and threshold results show a fabric where a zone of lighter elements has a higher spatial density likely along bedding, porosity also increases within these zones and decreases in the more homogenous dolomite-dominated zones.

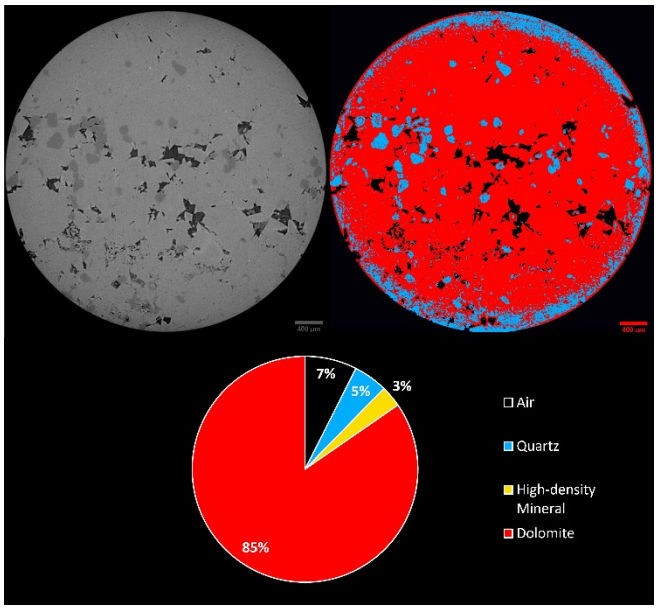

Fig. 9. Bonneterre-Reagan sand micro-Ct image (6,213.5 ft) with a slice of the volume showing the CT image unprocessed on left and segmentation results on right (400 µm scale is shown on the bottom right of both images) and below is a pie chart representing the portions of feature classes from the volume.

Bonneterre-Reagan Sandstone boundary at 6,213.50 ft (Fig. 9) was sampled just above the glauconitic sandstone that divides the Bonneterre and Reagan Sandstones. The sample is made up of dolomitic sand and represents a zone of increased porosity (9%) and permeability (about 0.1 mD). The Ilastik segmentation results, ignoring the outer 350 µm of the image due to beam-hardening effects, show the sample is primarily made up of dolomite (85%), quartz (5%), and high-density minerals (3%) with a porosity of 7%. The porosity in this sample is mostly located within the dolomitic sections of the rock with some propagating around the quartz grains. High-density minerals are generally about 10 µm or less through the volume apart from a 1 mm section of high-density mineral fill within the pore space towards the base of the CT volume.

The Reagan Sandstone at 6,222.60 ft (Fig. 10) was sampled from a section of medium-grained sandstone and has a porosity of 9% and a permeability of about 0.1 mD. The Ilastik segmentation results, ignoring the outer 400 µm due to beam-hardening effects, show the sample is primarily made up of dolomite (39.2%), feldspar (33.4%), quartz (17%), mineralized fracture-fill (5.4%), and high-density minerals (0.1%) with a porosity of 4.9%. Porosity in this sample is mostly within the dolomitic cement and surrounding the quartz grains, with minor amounts within intragranular fractures within feldspar grains.

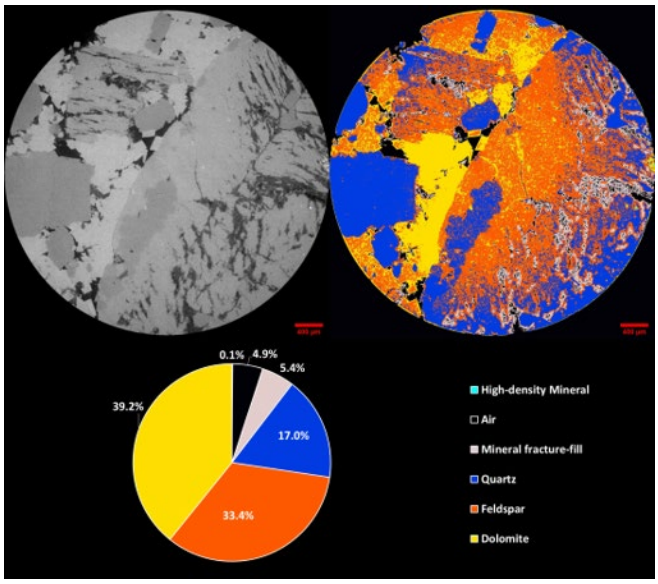

Fig. 10. Reagan Sandstone (6,222.60 ft) with a slice of the volume showing the CT image unprocessed on left and segmentation results on right (400 µm scale is shown on the bottom right of both images) and below is a pie chart representing the portions of feature classes from the volume.

4 Conclusions

Ilastik segmentation allows us to find mineralogy and porosity in a non-destructive manner. Heterogeneous samples create a challenge in dealing with beam-hardening effects at the sample edge. Our solution to this is to train the segmentation around the interior of the core where beam-hardening effects are minimized and create an ROI to ignore the areas where they are most prominent. This method is also limited to the number of samples investigated in this study. Ideally, we would have subsampled more to better represent each formation, however due to time constraints and longer scan times we weren't able to do so. In addition, the segmentation process can be tedious and sometimes takes weeks to come to a good solution. If a solution is found with minimum error, it can be used to train similar lithofacies.

Data from NETL coupled with core laboratory experiments and petrophysical logs allowed for the 625 feet of core from the Patterson #5-25 well to be assessed for reservoir quality at both the mm- and core-scale. We find reservoir potential in the Morrow Sand, Viola Formation, Upper Arbuckle, Lower Arbuckle, and Reagan Sand/Granite wash; and seals in the Atoka Stage, Meramecian Stage, and Osage Stage, as well as a baffle in the upper Bonneterre Formation. Core characterization analysis is summarized by the formation/group below:

Atoka Stage (4,615 to 4,751 ft) is a good seal with low porosity and permeability within the black shale and mudstone intervals and some thinner silty zones with moderate to high porosity and permeability.

Morrow Sand (4,751 to 4,880 ft) has the best reservoir quality within the Patterson #5-25 well with an average porosity of about 25% and permeability of 20 mD. The Morrow Sand is primarily made up of quartz sand with some minor amounts of clays and feldspars, and thinly bedded intervals of silt or mudrock. Micro-CT segmentation at 4,771.3 ft reiterates the findings at the core-scale. Porosity is about 20% and the sample is made up primarily of quartz. Porosity in the Morrow sample is found between sand grains with a minor seen within intragranular quartz and feldspar grains.

Meramecian Stage (4,880 to 4,957 ft) has seal potential with most of the mudstone intervals having low porosity and permeability and lack vertical fractures. However, there are vuggy intervals (4,869 to 4990 ft and 4,940 to 4,955 ft) within conglomerate and vuggy mudrock zones that have high porosity (12 to 15 %) and permeability (0.1 to 0.5 mD).

Osage Stage (5.380 to 5,439 ft) has seal potential. The upper 12 feet of the Osage core has the highest porosity and permeability and is made up of mudstone to packstone with intervals of chert. The tight section is made up of mudrock that has lower porosity and permeability. Coring missed the highest porosity interval observed in well logs, which suggests that the interval has good reservoir quality with approximately 10% porosity [2].

Viola Formation (5,640 to 5,719 ft) has reservoir potential, it is made up of dolopackstone with some zones of brecciation and chert. Zones of high porosity and permeability are present in vuggy areas and sections of pin-point pores with in the packstone.

Upper Arbuckle (5,780 to 5,826 ft) has reservoir potential with an average porosity of about 9% and permeability between 0.01 and 10 mD. The Upper Arbuckle is composed primarily of dolomudstone and dolograinstone. The highest porosity and permeability is found within the dolograinstones. The dolograinstones typically have more open vuggy and pinpoint porosity zones compared to the dolomudstones, which is chert-fill when present. Micro-CT segmentation of a dolograinstone interval at 5,812.4 ft showed the matrix is primarily made up of dolomite with very minor amounts of high-density minerals and quartz/feldspar grains, which were not captured in the segmentation. The sample was within the dolomite and had a porosity of 4.6% and vertical fracture sets.

Lower Arbuckle (5,959 to 6,200 ft) has200 ft) has good reservoir potential, in the Roubidoux Formation and lower Bonneterre Formation; and a baffle in the upper Bonneterre. The Roubidoux Formation high porosity and permeability zones are generally found in vuggy zones in doloboundstone and dolograinstone facies and sandy dolostone facies. Micro-CT segmentation of the Roubidoux Formation (5,972.12 ft) focused on a section of dolomudstone above a vuggy zone. The sample showed porosity mostly within heterogeneous zones with both dolomite and quartz/feldspar grains and had generally lower porosity than some other sections of the Roubidoux. The Bonneterre Formation high porosity zones are similarly found within vuggy zones on the doloboundstone facies and in sandy dolostone. Micro-CT segmentation of the sandy dolomitic facies at the Bonneterre-Reagan Sand boundary (6,213.5 ft) showed an increase in the proportion of dolomite to sand grains (in this case, quartz) compared to the sample in the Roubidoux Formation. However, porosity is higher (8.9%) and is made up of larger diameter pore space, propagating around the sand grains and within dolomite matrix. The baffle is also made up of dolomudstone and doloboundstone, however the section contains calcite-filled mineralized fractures.

Reagan Sand and Granite wash (6,214 to 6,273 ft) has reservoir potential, with porosity and permeability ranges between 9 to 15% and 0.01 and 10 mD. The Reagan Sand and Granite wash contain medium to fine-grained sandstones, siltstone, and conglomerates. The Reagan Sand is more dolomitic than the Granite wash which is more feldsparic. Micro-CT segmentation and analysis in The Reagan Sand focused on a sample from 6,222.60 ft that was made up of a medium grained dolomitic sandstone. The majority of the porosity in this sample is propagated around sand grains, with minor amounts from intragranular fracturing and within the dolomitic matrix. A couple qualitative observation can be made from the micro-CT segmentation. First, the porosity and likely permeability in the dolomitic sections is primarily from visible secondary porosity features (vugs, pin-point porosity, fractures) evident in the differences between core-scale measurements to the micro-CT result which are of mm-scale matrix. Second, porosity that is found in dolomitic rocks propagate more frequently in heterogenous sections of the sample compared to in the homogenous dolomite.

This observation could be made more robust with addition investigation in future studies. Such as, quantifying the pore space focusing on mineral contacts within the pore space important for wettability in CO_2 injection [11] and would show if heterogeneity is a significant factor in pore development. Exploring pore morphology (pore size and connectivity) is important for a deeper understanding of pressures needed for injection and in the cases of vuggy zones whether matrix pore space is connected for gas injection. the high-resolution digital rocks could be used to determined permeability and primary flow paths through the pore scape using computational fluid dynamics simulations, which could elucidate the role matrix plays in the dolomitic formations. Lastly, Taking the high-resolution pore-scale data from this experiment and understanding how to upscale and relate it to historic well data will be important moving forward.

Acknowledgement: The authors would like to acknowledge the NETL technical staff Karl Jarvis, Brian Tennent, and Scott Workman for providing the CT images in this report.
All data in this project is available on EDX (https://edx.netl.doe.gov/group/core-characterization).
This Research was executed through the NETL Research and Innovation Center's Carbon Storage field work proposal. Research performed by Leidos Research Support Team staff was conducted under the RSS contract 89243318CFE000003.

References

1. IPCC, Sustainable Development, and Efforts to Eradicate Poverty. https://www.ipcc.ch/sr15/, (2019)
2. J. Walker, K. Smith, Integrated Mid-Continent Stacked Carbon Storage Hub Phase II, Final Summary Report, DOE Agreement/Project #DE-FE0031623, Battelle Project # 100122657. (2020)
3. Y.E. Holubnyak, M. Dubois, Integrated CCS for Kansas (ICKan) Final Technical Report. No. DOE-ICKan-29474. Kansas Geological Survey; University of Kansas Center for Research (2018)
4. Kansas Geological Survey, Patterson Field " https://chasm.kgs.ku.edu/ords/oil.ogf4.IDProdQuery?FieldNumber=1000149180" (2022)
5. T. Paronish, N. Mitchell, R. Schmidt, J. Moore, S. Brown, D. Crandall, Computed Tomography Scanning and Geophysical Measurements of the Integrated Mid-Continent Stacked Carbon Storage Hub Patterson #5-25 Well, NETL-TRS-X-2021, NETL Technical Report Series (to be published)
6. Geotek Ltd. Multi-Sensor Core Logger Manual, Version 05-10, http://www.geotek.co.uk/sites/default/files/MSCLOverview.pdf, (2010)
7. J. Moore, S. Brown, D. Crandall, S. Workman, P. Dinterman, Computed Tomography of the Tuscarora Sandstone from the Preston 119 Well; NETL-TRS-9-2018; NETL Technical Report Series, 92, (2018)
8. S. Siddiqui, A. Khamees, Dual-Energy CT-Scanning Applications in Rock Characterization (SPE 90520). Society of Petroleum Engineers (2004)
9. C.A. Schneider, W.S. Rasband, K.W. Eliceiri, NIH Image to ImageJ: 25 years of image analysis. Nature Methods, 9, 671–675 (2012)
10. S. Berg, D. Kutra, T. Kroeger, C.N. Straehle, B.X. Kausler, C. Haubold, M. Schiegg, J. Ales, T. Beier, M. Rudy, and K. Eren, Ilastik: Interactive machine learning for (bio) image analysis. Nature Methods, 16, 1-7 (2019)
11. L. E. Dalton, D. Tapriyal, D. Crandall, A. Goodman, F. Shi, F. Haeri, Contact Angle Measurements Using Sessile Drop and Micro-CT Data from Six Sandstones. Transport in Porous Media, 133 (1), 71-83 (2020)